Catena 135 (2015) 290–303

Contents lists available at ScienceDirect

Catena

journal homepage: www.elsevier.com/locate/catena

The Late-Holocene geomorphic history of the Ethiopian Highlands: Supportive evidence from May Tsimble

Sil Lanckriet [a,*], Jean-Luc Schwenninger [b], Amaury Frankl [a], Jan Nyssen [a]

[a] University of Ghent, Department of Geography, Krijgslaan 281 (S8), B-9000 Ghent, Belgium
[b] University of Oxford, Research Laboratory for Archaeology and the History of Art, South Parks Road, OX13QY Oxford, UK

ARTICLE INFO

Article history:
Received 15 April 2015
Received in revised form 12 August 2015
Accepted 19 August 2015
Available online 2 September 2015

Keywords:
Alluvial sediments
Hydrogeomorphology
Land degradation
Political ecology

ABSTRACT

Alluvial sedimentary archives contain important geochronological and paleo-environmental information on past geomorphic processes in semi-arid regions. For North Ethiopia in particular, flashflood sediments transported by ephemeral streams can provide interesting chronological information on Late-Holocene land degradation, whether or not impacted by climate or land cover changes upstream. Here we compare geomorphic records with independent regional records of rainfall regime changes, land use/cover changes and macrohistory, supported by optically stimulated luminescence (OSL) dates for fluvial activity at a sediment sequence in the May Tsimble catchment, in the Northeastern Highlands. We identified two degradation periods over the past 4000 years, one broadly from 1500–500 BCE and one from 500 CE onwards. At least one prior incision phase is responsible for the stabilized gullies that can be seen on photographs around 1900 and another incision phase is dated to the late 20th century. Based on all datasets, we (re-)interpret the geomorphic history of the Highlands. Land degradation is dominantly determined by a human impact, although the impact of this human influence does get amplified during dry spells.

1. Introduction

In drylands worldwide, land degradation and desertification put severe pressure on food production and food security (Goudie, 2013). Deciphering the Late-Holocene history of land degradation forms an important aspect of a full understanding of the relative impacts of its (long-term) driving factors, including climate, land cover changes and sociopolitical impacts. River sediment yield and cycles of stream incision and deposition can provide suitable proxies for the intensity of land degradation (Avni et al., 2006; Lanckriet et al., 2014b; Vanmaercke et al., 2011, 2014), since erosion by ephemeral streams in drylands constitutes between 50 and 80% of all sediment production (Poesen et al., 2002). These sediments get accumulated or aggraded in alluvial floodplains, stored as valuable archives on Late-Holocene land degradation (Broothaerts et al., 2013).

We turn to the North Ethiopian Highlands, where severe gullying is indeed a major cause of land degradation (Frankl et al., 2013; Nyssen et al., 2004). Here, dense gully networks are present in the landscape (Frankl et al., 2011). However, few datasets exist on the Late-Holocene evolution of degradation processes in this region. Nyssen et al. (2009) showed that intense degradation occurred at least since the late 19th century, inferring a rather gradual environmental change. The oldest gully activity phase identifiable using repeat photography was a phase of relatively stable gullies that was evidenced on historical photographs of 1868–1936, lasting until the 1960s (Frankl et al., 2011, 2013). Hence, at a regional scale, Frankl et al. (2011) have identified one cut-and-fill cycle since the second half of the 19th century, and identified an earlier one based on the interpretation of historical photographs. Although at least one cycle had existed before 1868, the status of the gully networks that developed (and stabilized) before 1868 is unclear, since other hydrogeomorphic information on gullies before this period is lacking and no reliable direct sediment dating is available yet. A thorough chronological study on older cycles was never performed. It is hitherto not known if there is a continuous acceleration of geomorphic processes at longer time scales in the North Ethiopian Highlands. However, it is likely that the current cycle is the last of a series of cut-and-fill cycles, since driving factors were equally active during the previous centuries (Lanckriet et al., 2014b).

The sediments deposited by flashfloods in aggraded paleo-channels or preserved in terraces can also provide information on the driving factors of ephemeral stream systems. A literature review (Lanckriet et al., 2014b) shows that vegetation cover and climate changes are the two dominant driving factors of gullying named in most of the studies worldwide. Indeed, in the Ethiopian Highlands a decreasing vegetation cover upstream leads to intensified stream erosion and increased sediment supply downstream (aggradation) (Frankl et al., 2011). Simultaneously, Carnicelli et al. (2009) discuss the possibility that in the Ethiopian Highlands increased runoff under a wetter climate leads to overall gully incision; while decreased runoff and sediment

* Corresponding author.
E-mail address: sil.lanckriet@ugent.be (S. Lanckriet).

http://dx.doi.org/10.1016/j.catena.2015.08.011
0341-8162/

Table 1
Luminescence dating of ephemeral stream deposits all over the world. Only relevant papers (empirical research on Late Pleistocene or Holocene stream deposits) were incorporated in the review. Note that OD = Over Dispersion; IRSL = Infra-Red Stimulated Luminescence; and MAM = Minimum Age Model.

Cont	Country	Location	Sediments	Clim.	Is OSL suitable?	Solution	Age	OSL lab	Source
AM	Mexico	Oaxaca	Gully fluvial sands	Aw	No: paucity of quartz grains; incomplete bleaching	x	3.5 ka	Athens, USA	Leigh et al. (2013)
	USA	Southern Colorado	Arroyo	BSk	Partly: hetero-geneously bleaching	Single-grain model, single aliquot model	20 ka–0 ka	Oxford, UK	Arnold et al. (2007)
		Kanab Creek (Utah)	Arroyo sediments	Dsa	Incomplete bleaching if OD > 15% for small aliquots or OD > 25% for single-grains. Note that best OSL properties come from downstream reaches, ripple crossbeds or thin plane beds)	MAM-3 for small aliquots and MAM-4 for single-grain	6.7–3.5 ka	Utah State University Laboratory	Summa-Nelson and Rittenour (2012)
		Buckskin Wash (Utah)	Arroyo sediments and canyon paleofloods	Dsa	Incomplete bleaching	Single-grain analysis and MAM model	1.1–2.8 ka	Utah State University Laboratory	Harvey et al. (2011)
		California and Arizona	Arroyo channel sediments, infill and terrace	Csb and BSh	Incomplete bleaching	Non-logarithmic (unlogged) versions of CAM and MAM-3 or MAM-4 models	Modern and young samples (<350 years)	N/A	Arnold et al. (2009)
AF	Zambia	Chipata	Gully section	Aw, Cfa, Cwa	Yes	x	60 ka—Holocene	Roskilde, Denmark	Thomas and Murray (2001)
	Ethiopia	May Tsimble	Gully terraces	BSh	Yes	Residual age of modern sample	4 ka—now	Oxford (UK)	This study
	Tanzania	Irangi Hills	Gully fan	BSh	Heterogeneous bleaching	Minimum age model	900 and 600–300 BP	N/A	Eriksson et al. (2000)
	South Africa	Cape Point	Alluvial/colluvial fan	Csb	Yes	x	83–32 ka	Sheffield, UK	Shaw et al. (2001)
		Modder River	Alluvial gully (donga) infill	BSk	Incomplete bleaching	Minimum age model	0.39 ka	N/A	Tooth et al. (2013)
		Schoonspruit, Mooi, Klip	Floodplain deposits	Cwb	Incomplete bleaching (scatter in D_e or overdispersion OD > 20%)	Finite Mixture Model (or Central Age Model if OD < 20%	0.06–21.7 ka	Aberystwyth Laboratory	Keen-Zebert et al. (2013)
		KwaZulu-Natal (N)	Colluvial gully (donga) infill	Cwb	IRSL (K-feldspar)	No	Late Pleistocene	N/A	Botha et al. (1994)
AS	Israel	Negev Highland	Fluvio-loess (Pleistocene loess mobilized during flashfloods)	BW	Large errors due to residual OSL signal (incomplete bleaching)	x	45 ka–0.7 ka	N/A	Avni et al. (2012)
			Fluvio-loess / alluvium in ephemeral streams	BW	Yes for older deposits	Residual age of modern sample	70 ka to 0 ka	N/A	Avni et al. (2006)
	Mongolia	Upper Orkhon	Gully sediments	Dwb	Anomalous fading for K-feldspar dating; poor bleaching	Fading correction with g-value; Finite Mixture Model	0.7–15 ka	N/A	Lehmkuhl et al. (2011)
	Tibet	Tsangpo Valley	Gully terrace sediments	BSk	Partial bleaching if skew $>2\sigma_c$	Minimum Age Model	8.8–0.6 ka	N/A	Pelletier et al. (2011)
	China	Chifeng (Inner Mongolia)	Gully fan sediments	Dwa	Partial bleaching; coarse-grains are better bleached than fine-grains	Only using well-bleached samples	MIS 4-2	N/A	Avni et al. (2010)
		Gansu	Fluvially reworked loess in accumulation terraces	BWk	Yes (low scatter in D_e)	x	22.5–17.7 ka	N/A	Schütt et al. (2011)
		Jinsha River	Debris-flow	Cwa, Cwb	Yes	x	11 ka–4 ka	Bejing, China	Chen et al. (2008)
	Borneo	Western Kalimantan	Gully fill	Af	Scatter between aliquots (due to measuring procedure or incomplete bleaching	No	6–4 ka and 480 BP	UK	Teeuw et al. (1999)
EU	Germany	Franken	Gully sediments	Dfb	Partly: heterogeneous bleaching	Using (i) large quartz grains, (ii) Minimum Age Model, and (iii) single-grain analysis	Late Holocene	Liverpool, UK	Lang and Mauz (2006)

transport capacity under a dryer climate would increase the sediment supply downstream (aggradation). This is in line with the findings by Pelletier et al. (2011), who indicate that because of decreased runoff volumes, a drier climate is less capable of facilitating stream incision.

Obtaining reliable chronologies of stream activity is a key element for the acquisition of accurate environmental information on early land degradation intensities. This can be a particularly difficult task in drylands such as North Ethiopia, partly because ephemeral stream sediments are often not containing convenient organic matter to use for radiocarbon dating. Exceptionally, Machado et al. (1998) obtained an alluvial chronology for three sites in North Ethiopia using radiocarbon dating on buried paleosols. Optically stimulated luminescence (OSL) dating of flash flood sediments can be a valuable alternative, although it can suffer from insufficient or heterogeneous bleaching (Arnold et al., 2007; Bourke et al., 2003). OSL dating of relatively young sediments is also difficult given a low signal-to-noise ratio and processes such as thermic transfer (Costas et al., 2012; Eipert, 2004). A literature review regarding luminescence dating of ephemeral stream deposits all over the world (Table 1) shows that it is often possible to extract OSL ages from these flashflood sediments, although bleaching properties can strongly impact the level of accuracy. The review shows that most studies focusing on ephemeral stream sediments are dealing with heterogeneous bleaching properties (13 out of 20 studies). Solutions to this problem are given by residual age calculation, analysis of single grains or small aliquots and/or by applying the Minimum Age Model (MAM) of Galbraith et al. (1999) (7 out of the 13 studies). In this model, the (log) equivalent doses D_e form a random sample from a mixed truncated normal distribution. For (young) fluvial sediment samples, (un)logged MAM-3 or MAM-4 models are often preferred over other equivalent dose decision models, such as the Central Age Model, the L-5% model or the Finite Mixture Model (Bailey and Arnold, 2006). Some studies report bleaching properties dependent on grain size, with the coarsest quartz grains (e.g., 212–250 μm) yielding the lowest values of D_e (Alexanderson, 2007; Wallinga, 2002). Others employ a residual age calculation from a modern sample to empirically determine the age-overestimation due to poor bleaching (Table 1), as it is a very simple and straightforward method.

The aim of this study is to (re-)assess the Late-Holocene environmental evolution of the North Ethiopian Highlands using alluvial sedimentary archives. This can be done (i) by comparing geomorphic chronologies with other paleo environmental records from the region; and (ii) by bringing supportive evidence from dating of aggradation in a suitable catchment.

2. Methods

2.1. Geology of the study area and reconnaissance survey

The North Ethiopian Highlands drain toward the African Rift and the Tekeze–Nile rivers. The region is composed of Precambrian metavolcanics and Mesozoic sedimentary rocks, which include (from lower to upper) Adigrat sandstone, Antalo limestone, Agula shales, and Amba Aradam sandstone. These sedimentary rocks were intruded by younger (Cenozoic) dolerite dykes and sills and on top Tertiary basalts are found (Merla et al., 1979). Except for Enticho sandstone and the Adaga Arbi tillites, Paleozoic rocks are rare (Bussert and Schrank, 2007).

As it is wise to start with a mineralogical reconnaissance survey before turning to the luminescence procedures (Duller, 2008), several sites where observations had been done on the presence of old debris cones or (filled) paleo channels (Frankl et al., 2013) were visited during December 2012. Samples were taken at approximately 0.5 m depth in profile pits at interesting sediment accumulations in the main gullies, identified during walks around their catchments. Mineralogy of the sandy fraction (250–106 μm) was studied by microscope (Table 2). In the catchments of Nebelet and May Tsimble, in the uplands of the Rift Valley escarpment, sufficient quartz was present in the sediment samples (Table 2). As the stream system of May Tsimble is much more extensive compared to that of Nebelet, another fieldwork focused on the May Tsimble catchment. Downstream of the large upper stream network in May Tsimble (Fig. 1), an interesting sequence of terraces was identified in September 2013.

2.2. Review of paleo-environmental datasets

Available alluvial records were compared with independent paleo-environmental datasets from the region.

2.2.1. Hydroclimatic records

Two high-quality records of rainfall regime changes have been derived from sediment cores from Lake Ashenge (focus on BCE) (Marshall et al., 2009) and from Lake Hayk (focus on CE) (Lamb et al., 2007). At Lake Ashenge, the hydroclimatic record was derived from (i) diatom species analysis, (ii) diatom-inferred estimation of conductivity and (iii) stable oxygen and carbon isotope analysis of carbonates. At Lake Hayk, a similar methodology was used.

2.2.2. Land cover records

High-quality information of land cover changes was derived from pollen analysis of cores from Lake Hayk (Darbyshire et al., 2003) and pollen identification from Lake Ashenge (Marshall et al., 2009). At Lake Hayk, land cover was reconstructed from a combination of (i) pollen counting, (ii) pollen-assemblage zoning and (iii) the analysis of microscopic and macroscopic charcoal fragments.

2.2.3. Macrohistory

Macrohistory—the long-term patterns of political, economic and social change (Collins, 1999)—was derived from groundwork studies on the pre-Axumite period (Phillipson, 2009), on the Axumite period (Phillipson, 2012) and on the post-Axumite dynasties (Pankhurst, 1990). All reported dates are expressed in (B) CE ((Before) Common Era), including the calibrated radiocarbon dates derived from literature.

Table 2
Geology and mineralogy of the four catchments investigated during the reconnaissance survey.

Location	Sampled location (WGS84)	Geology of the catchment	Mineralogy of the sandy fraction (250–106 μm) in the sampled fill sediments
May Mekden	13.57834 °N, 39.57178 °E	Agula shales and Antalo limestone	90% micritic limestone fragments; 10% quartz; some zircon, sparitic calcite grains
Nebelet	14.12790 °N, 39.26888 °E	Enticho sandstone cliffs with underlying Precambrian metavolcanics	Nearly exclusively quartz; some opaque grains; mudstone fragments; possible plagioclase and microcline
May Tsimble	13.40372 °N, 39.67131°E	Antalo limestone with dolerite and sandstone near the water divide	Nearly exclusively quartz; some plagioclase and microcline; opaque grains
Ashenge	12.56571 °N, 39.51157 °E	Tertiary basalts (Ashangi group) and consolidated volcanic ashes	70% hornblende; 25% opaque grains; 5% plagioclase; some quartz, zircon, biotite, muscovite

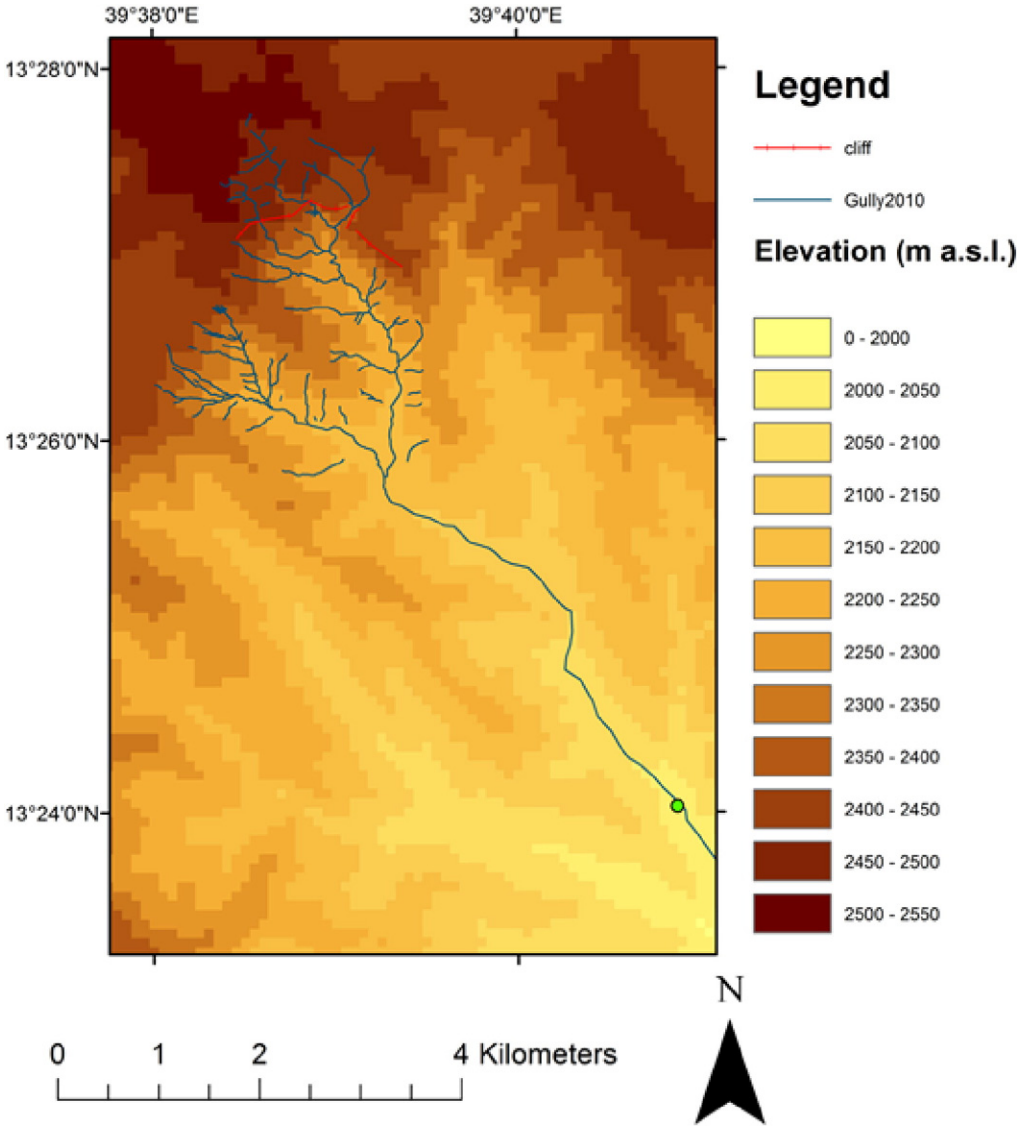

Fig. 1. Upper stream network in the May Tsimble catchment, upstream of our sampling site (indicated with green dot). For general localization of the catchment, see Fig. 5 (location C).

2.3. Supportive OSL evidence complemented with semi-structured interviews

2.3.1. Fieldwork, interviews and sampling

The May Tsimble catchment comprises a large ephemeral stream system about 20 km to the southeast of Mekelle, the capital city of the Tigray region in northern Ethiopia. Rainfall in the catchment likely ranges between 400–800 mm because of regional rainfall gradients and high relief. The sampling site (at around 2000 m a.s.l.) is located 6–8 km from the source of the stream, which is located in mountains rising to 2550 m a.s.l. Very recent flood deposits were observed at a height of 1.70 m above the channel floor, indicating the occurrence of individual flashflood events. The main stream is confined to a single ~3-m deep channel, with pool-riffle sequences cut into the alluvium until it reaches the underlying Antalo limestone bedrock. The channel width is about 9 m near the village of Lahama. The identified sequence of terraces is located at the left bank of the May Tsimble stream, along an abandoned palaeochannel next to the active channel (Fig. 2). Topographic heights and positions of all terraces were recorded (Fig. 2). In line with the method developed by Nyssen et al. (2006), we performed semi-structured interviews with 6 farmers, focusing on the stream evolution and the timing and processes of the changes in morphology. Samples for OSL dating were extracted from the terrace walls and in two profile pits (Fig. 2), in line with the recommendations of Duller (2008). For instance, we sampled at sandy lenses, used opaque tubes and wrapped them in thick black plastic. The sampled alluvial terraces are, similar to the contemporary bedload, mainly consisting of large sandy lenses with pebbles of dolerite, sandstone and limestone in-between. The sampling locations were chosen to include all alluvial terraces, in order to investigate the possibility of a complex terrace genesis instead of floodplain aggradation.

In order to estimate residual ages, one subrecent sample was collected from a sandy alluvium recently deposited just upstream of a new check dam built in 2010, 0.5 km upstream of the studied cross-section (Fig. 3).

2.3.2. Luminescence procedures

Measurements were performed at the Oxford University Luminescence Dating Laboratory on sand-sized quartz (180–255 μm) extracted from the seven samples (X6431–X6437) using standard preparation techniques including wet sieving, HCl (10%) treatment to remove carbonates, HF treatment (48%) to dissolve feldspathic minerals and heavy mineral separation with sodium polytungstate. All samples were measured in automated Risø luminescence readers

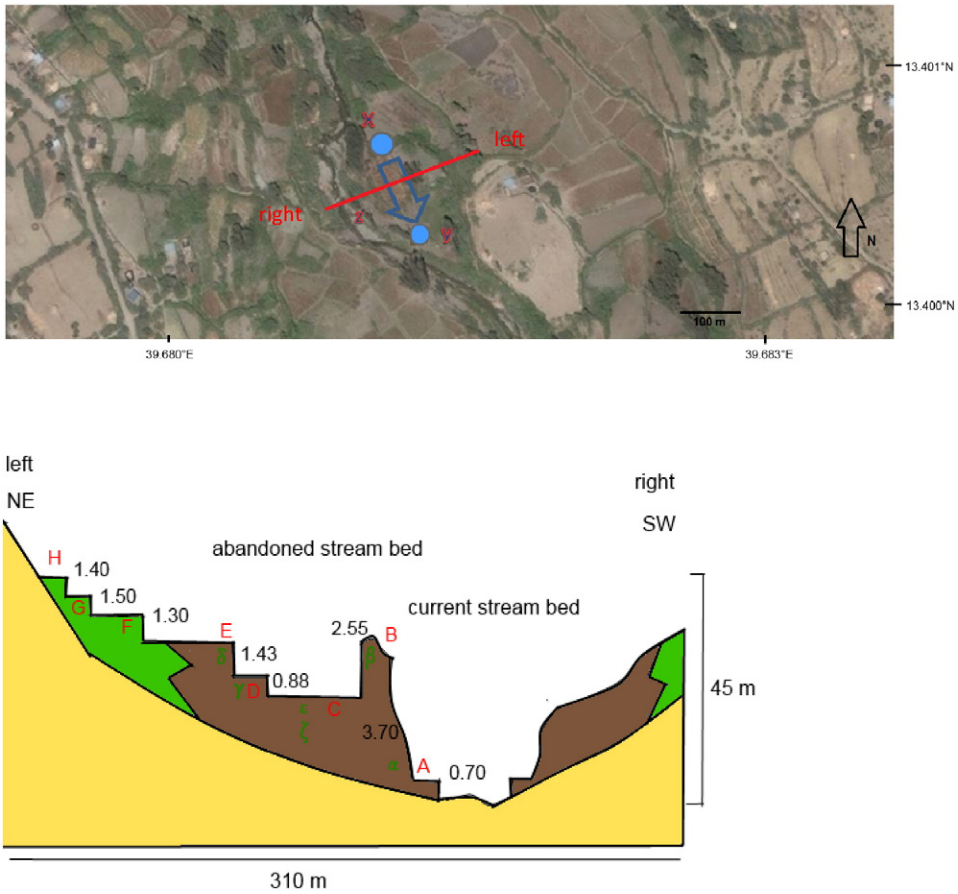

Fig. 2. Location of the study site from a BingMaps® satellite image with blue dots indicating the start and end of the paleo channel and the blue arrow indicating the paleo stream direction (up); and schematic profile of the study site with sequence of terraces (below) as indicated on the satellite image by red line, including relative heights (in m), coded terraces or locations (in red Latin letters) and OSL sample field codes (in green Greek letters). The Antalo limestone bedrock is indicated in yellow, colluvium in green and alluvium is indicated in brown. The inlet of the paleochannel (13.40114°N; 39.68072°E) is indicated with a letter X and the outlet is indicated with a letter Y (13.40050°N; 39.68125°E).

(Bøtter-Jensen, 1988, 1997; Bøtter-Jensen et al., 2000) using a SAR post-IR blue OSL measurement protocol (Banerjee et al., 2001; Murray and Wintle, 2000; Wintle and Murray, 2006). Dose rate calculations are based on the concentration of radioactive elements (potassium, thorium and uranium) within the samples and were derived from elemental analysis by Induced Coupled Plasma Mass Spectroscopy/Atomic Emission Spectroscopy using a fusion sample preparation technique. The final OSL age estimates include an additional 2% systematic error to account for uncertainties in source calibration. Dose rate calculations are based on Aitken (1985). These incorporated beta attenuation factors (Mejdahl, 1979), dose rate conversion factors (Adamiec and Aitken, 1998) and an absorption coefficient for the water content (Zimmerman, 1971). The contribution of cosmic radiation to the total dose rate was calculated as a function of latitude, altitude, burial depth

Fig. 3. Sampling site (indicated with red arrow) and sampling of the modern sample (M), just upstream of a newly built check dam in the May Tsimble channel.

Table 3
OSL data for single samples and aggradation depths (above the Antalo limestone base).

Description	Lab code and field code	Burial depth (cm)	Water content (%)	Paleodose (Gy)	±	Dose rate (Gy/ka)	±	OSL age (years before 2014)	Age after correction	±	Aggradation depth (above Antalo limestone base) (cm)
Residual age	X6431 (M)	34	13.3	0.48	0.2	1.22	0.07	<400	2010 CE		
Right upper terrace	X6432 (β)	150	13.6	0.27	0.24	1.45	0.07	<200	~1960 CE		474
Left upper terrace	X6433 (δ)	99	15.4	0.62	0.35	1.22	0.06	510	1804 CE	290	502
Top of the profile pit	X6435 (ε)	28	17.8	2.34	0.2	1.22	0.07	1920	394 CE	210	342
Left lower subterrace pit	X6434 (γ)	132	11.0	3.63	0.26	1.22	0.06	2970	656 BCE	270	326
Bottom of the aggradation	X6437 (α)	370	19.4	3.21	0.78	0.83	0.04	3860	1546 BCE	950	21
Bottom of the profile pit	X6436 (ζ)	120	14.5	27.27	4.98	1.09	0.05	24990	22676 BCE	4760	250

and average over-burden density based on data by Prescott and Hutton (1994). The OSL dates were then corrected with the average residual age of the modern samples and confronted with the vertical floodplain aggradation, based on the relative vertical position of the samples above the Antalo limestone bedrock (in cm).

3. Results

3.1. May Tsimble alluvial record

OSL age estimates (Table 3) are based on the concentration of radio-isotopes within the sample and include corrections for cosmic radiation and moisture content (Appendix A). Both the recent sample and the sample from the upper right terrace correspond to modern ages, which is consistent with the statements made by the interviewees. The other deposition dates range from 1846 ± 950 BCE to 1504 ± 290 CE. Despite the considerable errors due to the low sensitivity of the quartz, the dated sequence is consistent with the relative vertical position above the Antalo limestone bedrock. The dates point to a relatively simple genesis by floodplain aggradation instead of a more complex terrace genesis. One deposition date, sampled from the bottom of a profile pit, yielded a date of 22,976 ± 4760 BCE but this age estimate was strongly dependent upon the influence on the mean De estimate by a single outlier measurement. According to Wallinga (2002), the accuracy of OSL ages older than about 13 ka for such fluvial deposits can be dubious given the strong possibility of insufficient resetting at deposition and/or the inclusion of reworked older mineral grains having retained a residual signal (Duller, 2008). Because of this inconsistency this Pleistocene date was not considered.

We corrected the luminescence ages for an average residual age of 300 years (200–400 years for samples X6432 and X6431), an order of magnitude that is in line with findings by Porat et al. (2001). By confronting the dates with their vertical position above the bedrock, we calculated floodplain aggradation rates. We identify two broad periods of aggradation (Fig. 4). A first period of aggradation is dated ~1500 BCE till 500 BCE, followed by a period of low aggradation rates

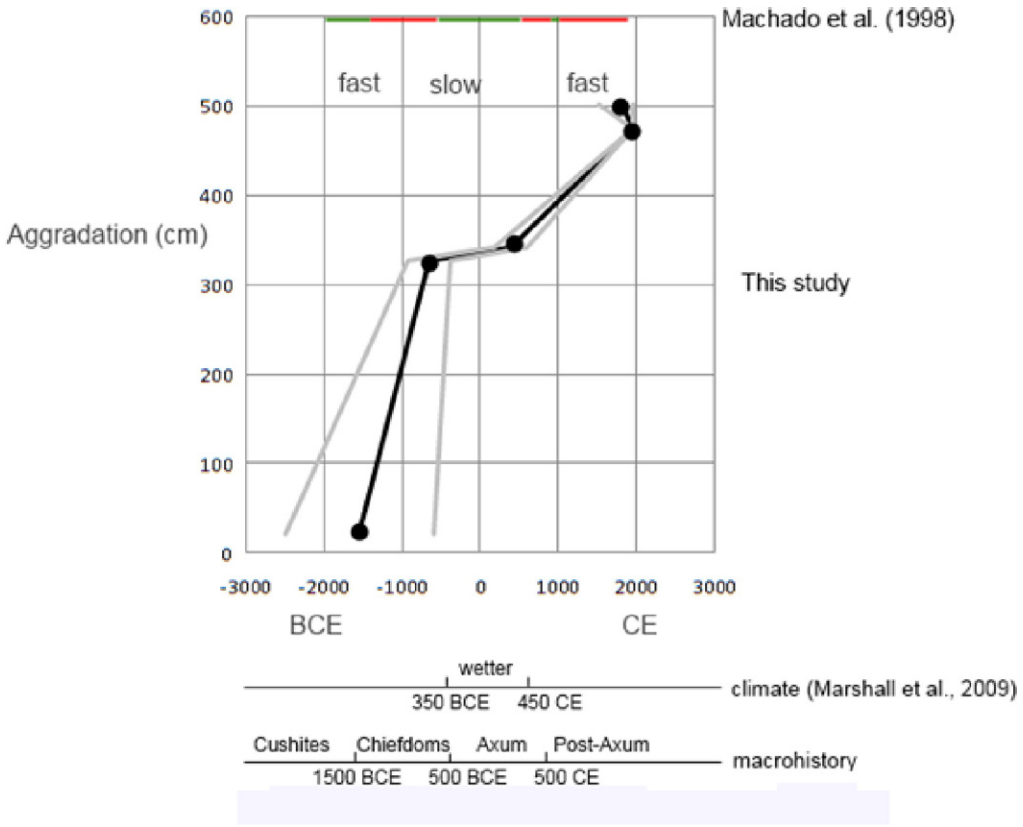

Fig. 4. Measured deposition ages (black dots) of sediment (BCE and CE) with errors (gray lines) as corrected for the residual age, and floodplain aggradation above the Antalo limestone base (cm) with indication of fast and slow aggradation rates. The degradation periods identified by Machado et al. (1998) are indicated with red bars, the vertisol stabilization periods are indicated with green bars. Important climatic and historical changes are also indicated.

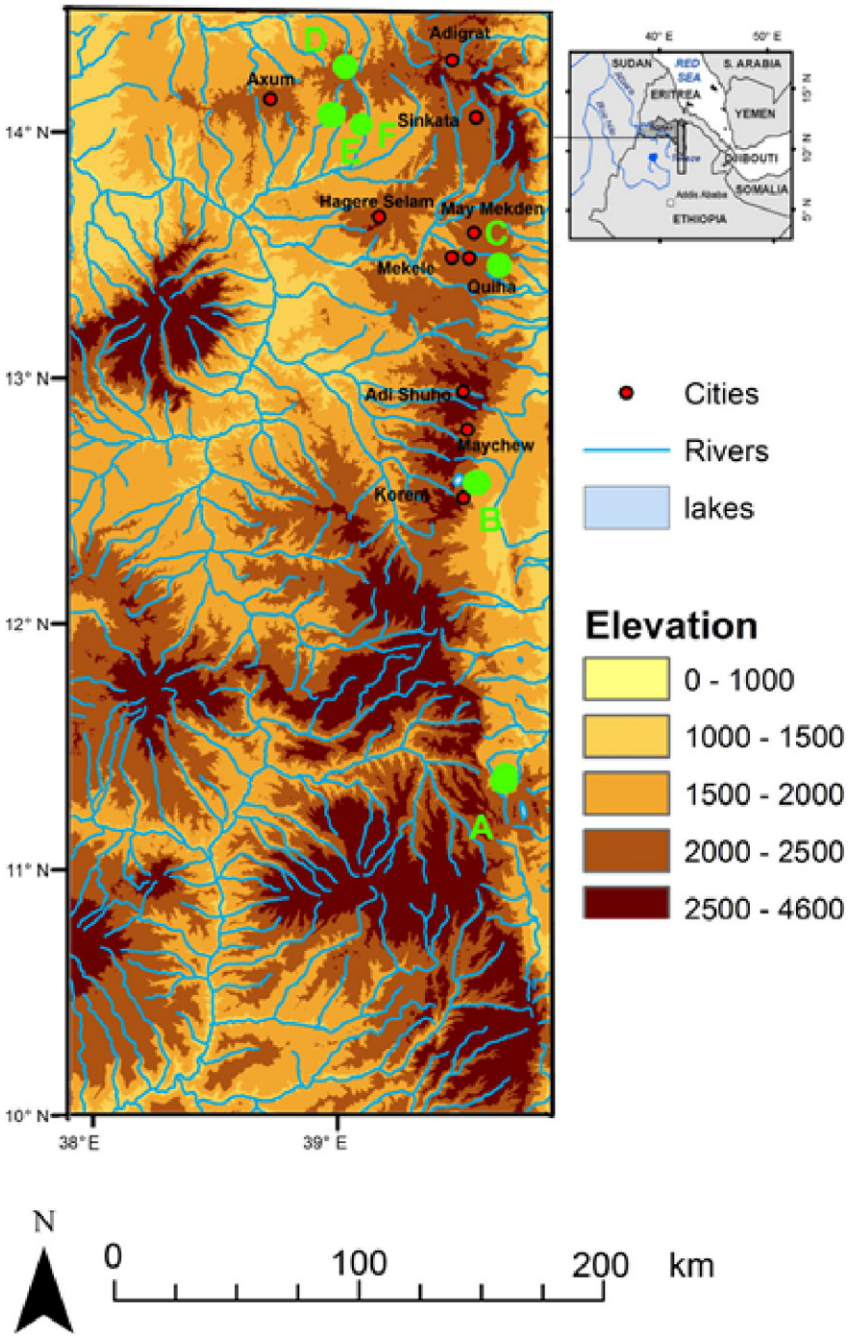

Fig. 5. Map of all mentioned paleo environmental records in the Northern Highlands, with A = Lake Hayk (Darbyshire et al., 2003; Lamb et al., 2007), B = Lake Ashenge (Marshall et al., 2009), C = May Tsimble (this study), D = Yeha (Pietsch and Machado, 2012), E = Adwa (Machado et al., 1998), F = Wechi and May Kinetal (Machado et al., 1998).

from ~500 BCE till 500 CE. A second phase of high aggradation rates starts from ~500 CE onwards.

3.2. Wechi, Adwa and May Kinetal alluvial records

Based on three records of infilled valley deposits (the Wechi record, the Adwa record and the May Kinetal record) (Fig. 5), Machado et al. (1998) identified three main stabilization periods over the past 4000 years (ca. 2000–1500 BCE, 500 BCE–500 CE and 950–1000 CE) with vertisol formation and three degradation episodes (ca. 1500–500 BCE, 500–950 CE, after 1000 CE) with increased sediment supply in Tigray. Because of the broad similarities with our record and the three records of Machado et al. (1998), we believe that the four records reflect a regional signal of altering geomorphic stability and degradation in the North Ethiopian Highlands. All the datasets confirm the occurrence of degradation periods during 1500–500 BCE and from 500 CE onwards. However, Machado et al. (1998) interpret these geomorphic degradation periods directly as phases of aridity, which should not necessarily be the case (Nyssen et al., 2004). Taking into account several independent high-quality paleoclimatic and palynological datasets obtained from lake cores in the region, a re-interpretation of these data is now proposed.

3.3. Correspondence with climate and land cover records

The paleoenvironmental records are schematized in Table 4 and localized on Fig. 5. Broadly, we follow the evidence from stable carbon isotope and elemental analyses (Terwilliger et al., 2011), showing that

Table 4
Regional rainfall regime changes and land cover changes in the North Ethiopian Highlands derived from Lake Hayk and Lake Ashenge; degradation derived from Wechi, Adwa, May Kinetal and May Tsimble; and macrohistory.

Rainfall regime		Land cover		Geomorphic activity		Macrohistory (e)		
3700-300 BCE	Relatively dry conditions after a wet period (5700-3700 BCE) (a)	Pre-500 BCE	Mixed conifer open forest (h), with first agriculture from 900 BCE (a)	2000-1500 BCE	Low (c, d)	3000 BCE – 800 BCE	Bronze Age and Punt/Kushitic Era, contact with Egypt	1000 BCE
				1500-500 BCE	High (c, d)	800-500 BCE	Pre-Axum, Damaat Era, Sabaean/Semitic immigration from Yemen	
300 BCE – 700 CE	Relatively dry (not dryer than present) (b) with shift to dryer conditions around 500 CE (a). No isotope evidence for increased wetness (a)	500 BCE – 1200 CE	First phase of strong deforestation from 500 BCE (h), intensified agriculture at 550 CE (a), intensified deforestation 900 CE (h)	500 BCE-500 CE	Low (c, d)	500 BCE – 1 CE	Proto-Axum	1 CE
						1 – 600 CE	Axumite Era, trade with Rome and South India	
				500 – 1000 CE	High (c, d)			
700-750 CE	Wet period (b), possibly lasting till 950 CE (a)					600-1000 CE	Fall of Axum under Arab expansion	
750-1200 CE	Dry "Medieval Warm Period" (a & b)			1000-1050 CE	Low (c)	1000-1300 CE	Centralized Zagwe Dynasty	1000 CE
				1050-1700 CE	High (c, d)			
1200-1700 CE	Wet "Little Ice Age", with small drought 1550 CE (b)	1200 - 1400 CE	Vegetation clearance to grasslands by grazing livestock (h)			1300-1600 CE	Moving, Roving Capitals; contact with Portugal, Oromo movements	1500 CE
		1400-1700 CE	Expansion of dry Afromontane forest (reforestation) (h)			1600-1700 CE	Renaissance and Rise of Gondar	
1700-1750 CE	Drying trend since 1650 (a) to 1675 CE (b), drought maximum 1750 CE (b) and wetter conditions after	1700 CE	Second phase of strong deforestation (h)	1700 – 2000 CE	Very high (c, d)	1700-1850 CE	*Zemene Mesafint*, period of decline, *gult* land tenure system	1700 CE
1750-2000 CE	Slightly wetter conditions after 1750 CE (with dryer early 19th century (f))	1860s-1930s	Increasing woody vegetation till the 1930s (g)			1850-1950	Centralization after Tewodros II, more trade	
		1940 -	Decline woody vegetation (g)			1950-1990	Military government	
		1990 - …	Increase woody vegetation (g)			Post 1990	TPLF government	

(a) Marshall et al. (2009); (b) Lamb et al. (2007); (c) Machado et al. (1998); (d) Our OSL datings; (e) Phillipson (2009), Phillipson (2012), Pankhurst (1990), Lanckriet et al. (2014a); (f) Nicholson et al. (2012); (g) Nyssen et al. (2014), (h) Darbyshire et al. (2003).

human land clearings have had the dominant impact on the Late-Holocene landscape in North Ethiopia as compared to climate changes. This is in line with the view of Connah (2001), who states in his review on African civilizations that the control of arable land and external trade are the two dominant factors determining this human impact in the Horn of Africa, by mediating the emergence of elites and states.

We constructed a conceptual geomorphic model (Fig. 6), under the reasonable assumption that aggradation periods correspond with phases of increased sediment supply from slopes into the valley, during phases of active degradation in the upper catchment. As a matter of fact, in North Ethiopian ephemeral streams decreasing woody vegetation cover following land clearings upstream leads to sediment accumulations downstream (Frankl et al., 2011). Indeed, following the equations of Frankl et al. (2011), channel aggradation (d^-) results from an increase in sediment supply (Q_s^+) (and/or a decrease in runoff Q^-). Simultaneously, channel incision (d^+) follows an increase in water runoff (Q^+) and/or a decrease in sediment load (Q_s^-). The earliest phase of incision might still be visible on historical photographs (late 19th century) and a second incision phase is attributed to the late 20th century (Fig. 6).

3.3.1. Geomorphic stability during the Cushitic era (before 1500 BCE)

After the dry Younger Dryas and the dry Early Holocene, precession-driven insolation changes initiated the African Humid Period (from 5650 BCE onwards) (Marshall et al., 2009). We identified tufa deposits in the main May Tsimble channel on a waterfall next to our study site (Fig. 7b), possibly referring to the stable hydrogeomorphic conditions at that time (Dramis et al., 2003; Moeyersons et al., 2006; Sagri et al., 2008). Pietsch and Machado (2012) found evidence of soil formation under an open woodland cover during this period (near Yeha, Tigray). Later, there was a shift to Late Holocene dryer conditions at ~3650 BCE, perhaps already starting from ~4000 BCE (Marshall et al., 2009). However, at the same time, the *Podocarpus–Juniperus* forest in the Northern Highlands was still intact (Darbyshire et al., 2003). Mixed forest including *Podocarpus*, *Juniperus*, *Celtis* and *Olea* covered the landscape, somewhat similar to the present montane forest of central Ethiopia (Darbyshire et al., 2003). During the 3rd and 2nd millennium BCE (Late Bronze Age), paleosols indicate environmental stability (Pietsch and Machado, 2012). Overall, the geomorphic stability during this period seems independent from the Late-Holocene shift to dryer conditions (4000–3650 BCE; Marshall et al., 2009).

3.3.2. Aggradation during the Pre-Axumite chiefdoms (1500–500 BCE)

At the base of our sequence (Fig. 7a), a first depositional unit was identified (Fig. 4, lower part). It represents about 300 cm of aggradation, deposited between 1500–500 BCE, corresponding with the first degradation period of Machado et al. (1998). The onset corresponds to the start of deforestation determined by Moeyersons et al. (2006), who date backfill and overfill deposits of tufa dams in Tigray from 1430–1260 BCE onwards. Pietsch and Machado (2012) identify slope degradation and high sediment yield during the second half of the 2nd millennium. Similarly, Bard et al. (2000) report increased sedimentation at the Meskilo River (near Mekele) after the early second millennium BCE.

Despite the absence of significant climate changes during this period (Marshall et al., 2009), these dates do match or closely follow the introduction of cattle herding from Sudan in the North Ethiopian Highlands, at the beginning of the 2nd millennium BCE (Lesur et al., 2014). Indeed,

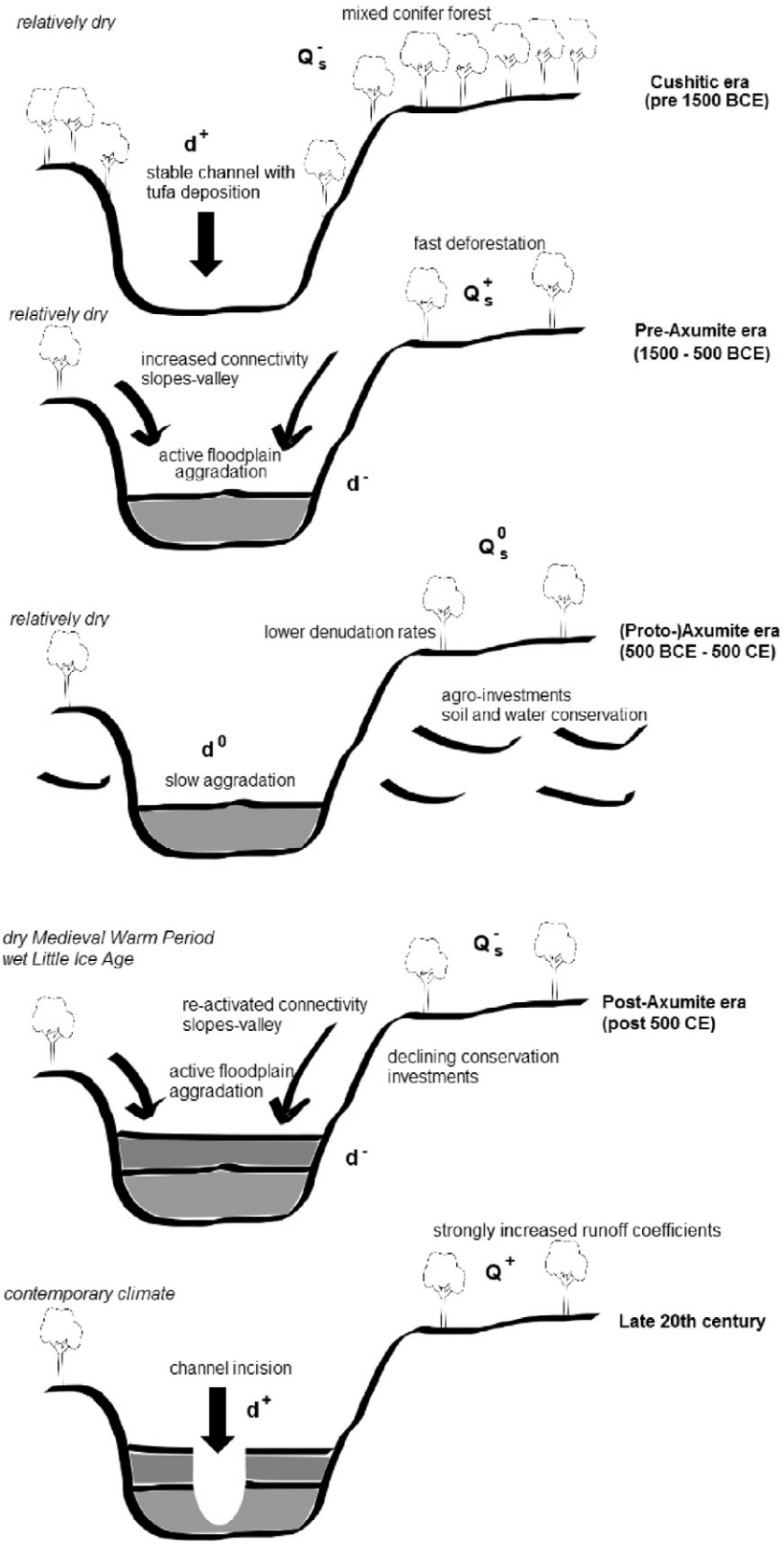

Fig. 6. Conceptual geomorphic model of stream and landscape evolution. The figure indicates channel aggradation (d^-), increase in sediment supply (Q_s^+), channel incision (d^+), increase in water runoff (Q^+) and a decrease in sediment load (Q_s^-). Indication of 0 stands for a stable situation.

the oldest evidence for domesticated cattle in North Ethiopia is dated to ~1800 BCE (Marshall and Negash, 2002). Simultaneously, during the 2nd millennium BCE, chiefdoms rose in the Ethiopian Highlands and in the Gash (D'Andrea et al., 2008). 'Pre-Axumite chiefdoms' might be the best term to describe these social organizations because, despite the existence of the Sabaean ruins of Yeha, there was never a centralized

Fig. 7. (a) Base of the sequence (indicated by stick) (left); and (b) small waterfall parallel to our study site, with travertine identified (indicated by red arrow) (right).

'Pre-Axumite state' (the so-called 'Damaat') (Phillipson, 2009). Pietsch and Machado (2012) identify decreased trees-to-shrub ratios over the Pre-Axumite times, as compared to the earlier Bronze Age.

More to the South (Lake Hayk), the timing of a rapid decline in *Podocarpus* and Cupressaceae forest is dated to 775–410 BCE (Darbyshire et al., 2003). At that time, the mixed conifer forest was replaced by disturbed, secondary bushland vegetation. Pollen evidence for this first large-scale deforestation concerns more than one taxon, indicating a dominant human interference, including vegetation clearance with the use of fire (Darbyshire et al., 2003). These large-scale deforestations happened about 600 years before deforestation in the Arsi and Bale Mountains (Hamilton, 1982), indicating a decreasing anthropogenic impact as one moves away from the Red Sea (Phillipson, 1985). Indeed, both the first deforestation and the high aggradation rates observed in May Tsimble by us, and in Wechi, Adwa and May Kinetal by Machado et al. (1998) coincide with migration of Semitic or Sabaean peoples from South Arabia toward Cushitic North Ethiopia, during the eighth and fifth century BC (Darbyshire et al., 2003).

3.3.3. Geomorphic stability during the (Proto-)Axumite state (500 BCE–500 CE)

Much slower aggradation rates were dated between 500 BCE and 500 CE, although no clear discordance was observed in the profiles. Compared to the faster aggradation before 500 BCE, this period comprising 16 cm of aggradation must represent a phase of geomorphological stability. The phase corresponds with the soil formation period described by Machado et al. (1998) (500 BCE–500 CE) and broadly coincides with the history of the Axumite state. French et al. (2009) indeed infer considerable landscape stability both during and prior to the Aksumite Period, evidenced by the development of vertic-like soils. In *The History*, Herodotos of Halicarnassos, 430 BCE (1862) describes Ethiopia as a very rich civilization. Following an explosion of demand for South Indian products in the Roman Empire (Rome, later Byzantium), there was a strong expansion of the Indian Ocean trade through the Red Sea, giving rise to the urban Axum Empire (Burstein, 2001; Phillipson, 2012). As reported in the *Periplus of the Erythraean Sea*, Adulis was an important sea port. The hegemony over the Red Sea and the Upper Nile ensured trade with Persians, Nubians and Yemen, while achieving the monopoly over trade routes to central Africa (D'Andrea et al., 2008). It can be assumed that increased resources allowed reducing pressure on the lands, as Bard et al. (2000) claim that no reduction in soil productivity can be found over the Axumite era. Pietsch and Machado (2012) identify increased trees-to-shrub ratios over the Axumite times, as compared to the Pre-Axumite period. Following Ciampalini et al. (2008), there are the Proto-Axumite (from ~450 BCE), Early Axumite (from ~90 BCE) and Classic Axumite (from ~100 CE) eras. Erosion rates in the immediate surroundings of Axum, calculated for these three main intervals are relatively low, proving the strong positive impact of Axum's extensive soil and water conservation (dams and terraces) (Ciampalini et al., 2008) and long-term landscape management by the growing population (French et al., 2009). However, this was a relatively dry period in the Highlands (Lamb et al., 2007). Generally, it is recognized that adoption and intensity of investments in water and soil conservation are positively dependent on land tenure security and farmers income (Kabubo-Mariara et al., 2006). During periods of social security, agricultural technology and intensification prosper while long-term conservation issues prevail over short-term survival (Nyssen et al., 2004). The impact of climate changes remains unclear but Marshall et al. (2009) suggest increased wetness in northern Ethiopia between 350 BCE and 450 CE.

3.3.4. Aggradation during the Post-Axumite era (500–1000 CE)

A second phase of faster aggradation rates was dated from 500 CE onwards, when more than 150 cm of sediment vertically filled the valley bottom. Since we did not measure sediment volumes, the vertical aggradation depth only gives an indication of the amount of deposited sediment—volumetric increase rate is assumed to be many times more important, given the triangular shape of the infilled valley bottom. Again, the ages correspond well with the degradation period (500–1000 CE) identified by Machado et al. (1998). At Lake Ashenge, pollen evidence points to an abrupt *Podocarpus* decline and enhanced soil erosion by 500 CE, under intensified land use (Marshall et al., 2009). Arab expansions from the 6th century onwards excluded Axum from the Indian Ocean trade system, leading to the chaotically post-Axumite era. Population continued to grow (McEvedy and Jones, 1978), deforestation progressed from 900 CE onwards (Darbyshire et al., 2003) and around 800 CE 'roving kingdoms' were rivaling over the Ethiopian plateau (Abebe, 1998) while famines and plagues culminated between 831–849 CE (Bard et al., 2000). The onset of this second aggradation period could coincide with a shift to a dryer climate around 500 CE (Marshall et al., 2009), but this shift was not identified at Lake Hayk and soon a wet period followed (700–750 CE) (Lamb et al., 2007), possibly lasting till 950 CE (Marshall et al., 2009).

3.3.5. Possible geomorphic stability under the Zagwe state (1000–1150 CE)

Machado et al. (1998) identified another period of low sediment activity (calibrated dates from 1013–1164 CE), which could have been left undetected in the May Tsimble record given its lower resolution. Brancaccio et al. (1997) also report on pedogenesis around 700 and 980 CE. This Medieval Warm Period (750–1200 CE) is in North

Ethiopia relatively dry (Lamb et al., 2007). However, the centralized Zagwe rule (1000–1250 CE) based in the Lasta region, was rather peaceful, stable and urban and was involved in long-distance trade from the port of Zayla (Pankhurst, 1997; Negash, 2006). More datasets are required to investigate the specificities of human–environment interactions at that time.

3.3.6. Aggradation during the 'Early Medieval Times'

A third phase of faster aggradation rates was reported by Machado et al. (1998) after 1050 CE. As the stabilization phase discussed above (~1000–1050 AD) was undetected in the May Tsimble record, these faster aggradation rates are there dated from 500 CE onwards. However, the 'Little Ice Age' was quite wet in North Ethiopia, characterized by another wet interval around 1300 CE and a small drought around 1550 CE (Lamb et al., 2007). By contrast, following intensification of grazing, grasslands were expanding around 1200–1400 CE (Darbyshire et al., 2003). European historical sources from the 'Early Medieval times' report on vast amounts of cattle and grasslands under large-scale deforestation in Ethiopia (Pankhurst, 1990). There were frequent civil wars with rebelling vassals or Muslim lowlanders during this unstable Solomonic dynasty. Lands were owned by noblemen or by the Church while reported in *Il Milione* by Marco Polo (from second hand information), trade was dominated by Arabs (and some Armenians). Instead of a fixed capital, there were 'moving camps', and there are many reports on crop plagues by locusts and rats (Pankhurst, 1990).

3.3.7. Late Medieval reforestation

During the 'Late Medieval times', Darbyshire et al. (2003) identified a gradual reforestation of *Juniperus*-dominated dry Afromontane forest between 1400 and 1700 CE. Following the war between the Adal Sultanate and Ethiopia and Portugal, Oromo peoples moved to the Highlands and their nomadic pastoralism reduced pressure on the land (Darbyshire et al., 2003). Portuguese reports state fewer cattle in the early 16th (Thomas of Angot) and 17th century (Manuel de Almeida) (Pankhurst, 1990). Under the new capital of Gondar (1632) and commercialization of agriculture, the late 17th century was an urban period of renaissance, trading with Sudan and from the port of Massawa (Pankhurst, 1990). The rise of Gondar occurred despite a drying trend since 1650 CE (Lamb et al., 2007). Little information on geomorphic activity is available for this period, although a phase of soil formation has been dated up to 1641 AD in Adi Kolen (Bard et al., 2000). It must be noted that such periods of soil formation can also result from a particular local evolution of vegetation cover (Nyssen et al., 2004), so again more data must be gathered to identify spatial-regional patterns. Also note the possibility that the stabilized channel incisions that are visible on 19th-century terrestrial photographs (see Frankl et al., 2011) result from a *clear water effect* under an increased Late Medieval vegetation cover.

3.3.8. The 20th century

Finally, according to the semi-structured interviews with farmers around our study site, the May Tsimble stream incised and shifted its channel to the right (i.e., to the West) around the 1960s–1970s. Gully incision has been observed at regional scale during this period (Frankl et al., 2011, 2013). In the modern channel, very recent re-incision is visible as a small intra-channel terrace. It might be the result of a clear-water effect after the large-scale implementation of conservation measures (including the dam pictured in Fig. 3), following increased sediment supply during the 1960s–1980s. These phases correspond well with the three main geomorphic periods over the 20th century identified by Lanckriet et al. (2014a) and Frankl et al. (2011). There is the *feudal era*, with some widely implemented conservation structures (such as *dagets*) (Lanckriet et al., 2014a), quite stable channels with an oversized inherited morphology and low sediment supply (Frankl et al., 2011). Following strongly increased runoff coefficients, a general incision phase was documented to start in the (late feudal) 1960s. It continued through the civil war as strengthened by the effect of droughts and a lack on investments in conservation during the 1980s (Frankl et al., 2011). Finally, there is the *post-war era*, with new conservation efforts, more equal land rights (Lanckriet et al., 2014a) and again lower sediment supply and lower runoff response (Frankl et al., 2011).

4. Discussion

Periods of stronger geomorphic activity do not directly coincide with periods of increased aridity; although this does not strictly imply that more indirect or nonlinear climate–land interactions did not occur.

Geomorphic stability is for instance present under both dry and wet conditions. Low geomorphic activity before 1500 BCE is not in phase with the much earlier shift to dryer conditions (3650 BCE; Marshall et al., 2009). The same is true for the first wave of large-scale deforestation during the second-first millennium BCE (Darbyshire et al., 2003). Geomorphic stability matching the emergence of the (Proto-)Axumite state (broadly from 500 BCE to 500 CE) (French et al., 2009) occurred during a relatively dry period (Lamb et al., 2007). Note that the diatom evidence from the Lake Ashenge record suggesting increased wetness between 200 BCE–500 CE is not evidenced by stable isotopes (Marshall et al., 2009). A period of lower sediment supply dated to 1013–1164 CE (Machado et al., 1998) happened during the relatively dry Medieval Warm Period (Lamb et al., 2007) while relatively high geomorphic activity in the Highlands from 1050 to 1700 CE coincides with the wetter Little Ice Age.

Land cover records further indicate three waves of deforestation and subsequent reforestation in the Highlands, suggesting but not clearly exhibiting a link with dry or wet periods. A *Podocarpus–Juniperus* forest dominated the Highlands before the first millennium BCE, while the earliest pollen evidence for forest decline in the Ethiopian Highlands was linked with Semitic immigrations instead of drought (Darbyshire et al., 2003). Thereafter scrub and grassland vegetation persisted for about 1800 years; with a specific dominance of grasslands from ~1200 to 1400 CE (Darbyshire et al., 2003). Despite the dominance of scrub and grassland vegetation from 500 BCE to 500 CE, the landscape was relatively stable (French et al., 2009). Forest regrowth then did occur during the wet Little Ice Age as *Juniperus*, *Olea* and *Celtis* forest extent increased again from 1400 to 1700 CE (Darbyshire et al., 2003; Lanckriet et al., in press). The second phase of large-scale deforestation during the dry 18th century was evidenced from pollen analysis by Darbyshire et al. (2003) and by Lanckriet et al. (in press), who identified an 18th century decline in *Olea*, *Celtis* and *Podocarpus* under an increase in Poaceae pollen. Consequently, the Northern Ethiopian Highlands were heavily deforested in the 19th century (Nyssen et al., 2009) when already considerable runoff was produced (Lanckriet et al., 2014b). A minimal woody vegetation cover persisted from the 1950s to the 1990s (Lanckriet et al., in press), overlapping with the dry decade of the 1980s, but a new period of increased forest extent is evident over the last two decades (Nyssen et al., 2014). Nyssen et al. (2009) hence show that nowadays, instead of total degradation, an increase of woody biomass can be observed.

Finally it is worth mentioning that long-term and extreme dry conditions in the Highlands are a relatively rare phenomenon. The isotope record from Lake Hayk shows that the regional climate during the last two millennia was generally always moister than at present, with only two exceptions (a phase around 800 CE and from 1750 to 1880 CE) (Lamb et al., 2007).

5. Conclusions

In this study, we reviewed a number of paleo environmental records from the North Ethiopian Highlands and additionally used optically stimulated luminescence to date aggradation phases in the May Tsimble

catchment (North Ethiopia). Preceded and interrupted by periods of low aggradation rates, we identified two periods of faster alluvial deposition in the catchment, from 1500–500 CE and after 500 CE. The results are consistent with radiocarbon dating results from the Wechi, Adwa and May Kinetal catchments. We infer that the sequence of terraces in May Tsimble is resulting from two depositional phases, followed by recent incision. Stable channels observable on mid-19th-century terrestrial photographs indicate at least one earlier incision phase. Comparison with independent records from lake sediments shows that periods of faster aggradation do not correspond directly with periods of increased aridity or wetness. There is however a clear dominant human impact, as the first degradation phase coincides with the introduction of cattle herding and the second phase with the post-Axumite era. The Late-Holocene history of geomorphic activity in the Ethiopian Highlands, often interpreted as directly driven by climate, bears imprints of investments in soil and water conservation during periods of social chaos.

Acknowledgments

This study would not have been possible without the enormous support, friendship and help of our translator Gebrekidan Mesfin, the important input on mineralogy from Florias Mees, the advice from Dimitri Vandenberghe, the support and kindliness of the farmers near the study site, the kind hospitality of the Luminescence Dating Laboratory of the University of Oxford, the funding of UGent Special Research Fund (number UG_3531759700), as well as the logistical support through Belgian VLIR projects at Mekelle University (IUC and Graben TEAM).

Appendix A

K, Th and U concentrations, as determined by Induced Coupled Plasma Mass Spectroscopy/Atomic Emission Spectroscopy using a fusion sample preparation technique.

	Unit	X6431	X6432	X6433	X6434	X6435	X6436	X6437
Grain sizes								
Min. grain size	(mm)	180	180	180	180	180	180	180
Max. grain size	(mm)	255	255	255	255	255	255	255
Measured concentrations								
Standard fractional error	(%)	5	5	5	5	5	5	5
% K	(%)	0.697	0.905	0.672	0.706	0.755	0.64	0.43
Error (% K)	(%)	0.035	0.045	0.034	0.035	0.038	0.032	0.022
Th	(ppm)	3	4.3	3.5	3.1	3.4	2.9	2.3
Error (Th)	(ppm)	0.15	0.215	0.175	0.155	0.17	0.145	0.115
U	(ppm)	1.1	1.3	1.3	1.1	1.1	1	1.2
Error (U)	(ppm)	0.055	0.065	0.065	0.055	0.055	0.05	0.06

Equivalent doses, cosmic doses, moisture content, total dose rate and age estimates.

	Unit	X6431	X6432	X6433	X6434	X6435	X6436	X6437
De	(Gy)	(0.48)	(0.27)	0.62	3.63	2.34	27.27	3.21
Uncertainty		0.19	0.24	0.35	0.27	0.21	5.01	0.77
Cosmic dose calculations								
Depth	(m)	0.34	1.5	0.99	1.32	0.28	1.2	3.7
Error	(m)	0.05	0.05	0.05	0.05	0.05	0.05	0.05
Average overburden density	($g.cm^3$)	1.9	1.9	1.9	1.9	1.9	1.9	1.9
Error	($g.cm^3$)	0.1	0.1	0.1	0.1	0.1	0.1	0.1
Latitude		13	13	13	13	13	13	13
Longditude		40	40	40	40	40	40	40
Altitude	(m a.s.l.)	2052	2023	2023	2020	2020	2019	2019
Geomagnetic	latitude	9	9	9	9	9	9	9
Dc	(Gy/ka), 55 N G.lat, 0 km Alt.	0.201	0.172	0.184	0.176	0.202	0.179	0.131
Error		0.033	0.014	0.016	0.014	0.039	0.015	0.01
Cosmic dose rate	(Gy/ka)	0.249	0.213	0.228	0.218	0.25	0.222	0.162
Error	0.041	0.017	0.02	0.018		0.048	0.019	0.012
Moisture content								
Measured water	(% of wet sediment)	13.27	13.64	15.38	11	17.78	14.54	19.36
Moisture	(water/wet sediment)	0.13	0.14	0.15	0.11	0.18	0.15	0.19
Error	0.03	0.03	0.03	0.03		0.03	0.03	0.03
Total dose rate	(Gy/ka)	1.216	1.449	1.216	1.224	1.218	1.091	0.831
Error		0.07	0.075	0.06	0.062	0.075	0.054	0.039
OSL age estimate	(yr before 2014)	(<400)	(<200)	510	2970	1920	24990	3860
Error				290	270	210	4760	950

References

Abebe, B., 1998. Histoire de L'Éthiopie d'Axoum à la revolution. Maisonneuve et Larose, Paris.
Adamiec, G., Aitken, M.J., 1998. Dose–rate conversion factors: new data. Ancient TL 16, 37–50.
Aitken, M.J., 1985. Thermoluminescence Dating. Academic Press, New York.
Alexanderson, H., 2007. Residual OSL signals from modern Greenlandic river sediments. Geochronometria 26, 1–9.
Arnold, L., Bailey, R., Tucker, G., 2007. Statistical treatment of fluvial dose distributions from southern Colorado arroyo deposits. Quat. Geochronol. 2, 162–167.
Arnold, L., Roberts, R., Galbraith, R., DeLong, S., 2009. A revised burial dose estimation procedure for optical dating of young and modern-age sediments. Quat. Geochronol. 4, 306–325.
Avni, Y., Porat, N., Plakht, J., Avni, G., 2006. Geomorphic changes leading to natural desertification versus anthropogenic land conservation in an and environment, the Negev Highlands, Israel. Geomorphology 82 (3–4), 177–200.
Avni, Y., Zhang, J., Shelach, G., Zhou, L., 2010. Upper Pleistocene–Holocene geomorphic changes dictating sedimentation rates and historical land use in the valley system of the Chifeng region, Inner Mongolia, northern China. Earth Surf. Process. Landf. 35 (11), 1251–1268.

Avni, Y., Porat, N., Avni, G., 2012. Pre-farming environment and OSL chronology in the Negev Highlands, Israel. J. Arid Environ. 86, 12–27.
Bailey, R., Arnold, L., 2006. Statistical modelling of single grain quartz D-e distributions and an assessment of procedures for estimating burial dose. Quat. Sci. Rev. 25 (19–20), 2475–2502.
Banerjee, D., Murray, A.S., Bøtter-Jensen, L., Lang, A., 2001. Equivalent dose estimation using a single aliquot of polymineral fine grains. Radiat. Meas. 33, 73–94.
Bard, K., Coltorti, M., Di Blasi, M., Dramis, F., Fattovich, R., 2000. The environmental history of Tigray (Northern Ethiopia) in the Middle and Late Holocene: a preliminary outline. Afr. Archaeol. Rev. 17 (2), 65–86.
Botha, G., Wintle, A., Vogel, J., 1994. Episodic Late Quaternary palaeogully erosion in Northern Kwazulu Natal, South Africa. Catena 23 (3–4), 327–340.
Bøtter-Jensen, L., 1988. The automated Risø TL dating reader system. Nucl. Tracks Radiat. Meas. 14, 177–180.
Bøtter-Jensen, L., 1997. Luminescence techniques: instrumentation and methods. Radiat. Meas. 27, 749–768.
Bøtter-Jensen, L., Bulur, E., Duller, G.A.T., Murray, A.S., 2000. Advances in luminescence instrument systems. Radiat. Meas. 32, 523–528.
Bourke, M., Child, A., Stokes, S., 2003. Optical age estimates for hyper-arid fluvial deposits at Homeb, Namibia. Quat. Sci. Rev. 22, 1099–1103.
Brancaccio, L., Calderoni, G., Coltorti, M., Dramis, F., 1997. Phases of soil erosion during the Holocene in the Highlands of Western Tigray (Northern Ethiopia): a preliminary report. In: Bard, K. (Ed.), The Environmental History and Human Ecology of Northern Ethiopia in the Late Holocene. Instituto Universitario Orientale, Napoli, pp. 30–48.
Broothaerts, N., Verstraeten, G., Notebaert, B., Assendelft, R., Kasse, C., Bohncke, S., Vandenberghe, J., 2013. Sensitivity of floodplain geoecology to human impact: a Holocene perspective for the headwaters of the Dijle catchment, central Belgium. The Holocene 23 (10), 1403–1414.
Burstein, S., 2001. State formation in ancient Northeast Africa and the Indian Ocean Trade. Conference Proceeding of the American Historical Association: Interactions, Regional Studies, Global Processes, and Historical Analysis: 28 February 2001. Library of Congress, Washington D.C. (Accessed on 02 December 2014 and available from: http://webdoc.sub.gwdg.de/ebook/p/2005/history_cooperative/www.historycooperative.org/proceedings/interactions/burstein.html).
Bussert, R., Schrank, E., 2007. Palynological evidences for a latest Carboniferous–Early Permian glaciation in Northern Ethiopia. J. Afr. Earth Sci. 49, 201–210.
Carnicelli, S., Benvenuti, M., Ferrari, G., Sagri, M., 2009. Dynamics and driving factors of late Holocene gullying in the Main Ethiopian Rift (MER). Geomorphology 103 (2), 541–554.
Chen, J., Dai, F., Yao, X., 2008. Holocene debris-flow deposits and their implications on the climate in the upper Jinsha River valley, China. Geomorphology 93 (3–4), 493–500.
Ciampalini, R., Billi, P., Ferrari, G., Borselli, L., 2008. Plough marks as a tool to assess soil erosion rates: a case study in Axum (Ethiopia). Catena 75, 18–27.
Collins, R., 1999. Macrohistory: Essays in Sociology of the Long Run. Stanford University Press, Redwood City, USA (312 pp.).
Connah, G., 2001. African Civilizations: An Archaeological Perspective. Cambridge University Press (340 pp.).
Costas, I., Reimann, T., Tsukamoto, S., Ludwig, J., Lindhorst, S., Frechen, M., Hass, H., Betzler, C., 2012. Comparison of OSL ages from young dune sediments with a high-resolution independent age model. Quat. Geochronol. 10, 16–23.
D'Andrea, C., Manzo, A., Harrower, M., Hawkins, A., 2008. The Pre-Aksumite and Aksumite settlement of NE Tigrai, Ethiopia. J. Field Archaeol. 33, 151–176.
Darbyshire, I., Lamb, H., Umer, M., 2003. Forest clearance and regrowth in northern Ethiopia during the last 3000 years. The Holocene 13, 537–546.
Dramis, F., Umer, M., Calderoni, G., Haile, M., 2003. Holocene climate phases from buried soils in Tigray (northern Ethiopia): comparison with lake level fluctuations in the Main Ethiopian Rift. Quat. Res. 60, 274–283.
Duller, G., 2008. Luminescence Dating: Guidelines on Using Luminescence Dating in Archaeology. English Heritage, Swindon.
Eipert, A., 2004. Optically Stimulated Luminescence (OSL) Dating of Sand Deposited by the 1960 Tsunami in South-central Chile. Geology Comps Papers.
Eriksson, M., Olley, J., Payton, R., 2000. Soil erosion history in central Tanzania based on OSL dating of colluvial and alluvial hillslope deposits. Geomorphology 36 (1–2), 107–128.
Frankl, A., Nyssen, J., De Dapper, M., Haile, M., Billi, P., Munro, N., Deckers, J., Poesen, J., 2011. Linking long-term gully and river channel dynamics to environmental change using repeat photography (Northern Ethiopia). Geomorphology 129, 238–251.
Frankl, A., Poesen, J., Scholiers, N., Jacob, M., Haile, Mitiku, Deckers, J., Nyssen, J., 2013. Factors controlling the morphology and volume (V)–length (L) relations of permanent gullies in the Northern Ethiopian Highlands. Earth Surf. Process. Landf. 38, 1672–1684.
French, C., Sulas, F., Madella, M., 2009. New geoarchaeological investigations of the valley systems in the Aksum area of northern Ethiopia. Catena 78 (3), 218–233.
Galbraith, R., Roberts, R., Laslett, G., Yoshida, H., 1999. Optical dating of single and multiple grains of quartz from Jinmium rock shelter, Northern Australia: Part I, experimental design and statistical models. Archaeometry 41 (2), 339–364.
Goudie, A., 2013. The Human Impact on the Natural Environment: Past, Present, and Future. John Wiley and Sons, Hoboken, New Jersey.
Hamilton, A., 1982. Environmental History of East Africa. Academic Press, London (328 pp.).
Harvey, J., Pederson, J., Rittenour, T., 2011. Exploring relations between arroyo cycles and canyon paleoflood records in Buckskin Wash, Utah: reconciling scientific paradigms. Geol. Soc. Am. Bull. 123 (11–12), 2266–2276.
Herodotos of Halicarnassos, 430 BCE, 1862. The Histories: Muse 3, 114.1. The History. Dutton, New York (trans. George Rawlinson).
Kabubo-Mariara, J., Linderhof, V., Kruseman, G., Atieno, R., Mwabu, G., 2006. Household Welfare, Investment in Soil and Water Conservation and Tenure Security: Evidence From Kenya. PREM Working Paper: PREM 06/06.
Keen-Zebert, A., Tooth, S., Rodnight, H., Duller, G., Roberts, H., Grenfell, M., 2013. Late Quaternary floodplain reworking and the preservation of alluvial sedimentary archives in unconfined and confined river valleys in the eastern interior of South Africa. Geomorphology 185, 54–66.
Lamb, H., Leng, M., Telford, R., Ayenew, Tenalem, Umer, M., 2007. Oxygen and carbon isotope composition of authigenic carbonate from an Ethiopian lake: a climate record of the last 2000 years. The Holocene 17 (4), 517–526.
Lanckriet, S., Derudder, B., Naudts, J., Araya, Tesfay, Cornelis, W., Bauer, H., Deckers, J., Haile, Mitiku, Nyssen, J., 2014a. A political ecology perspective of land degradation in the North Ethiopian Highlands. Land Degrad. Dev. 26 (5), 521–530.
Lanckriet, S., Frankl, A., Descheemaeker, K., Mesfin, Gebrekidan, Nyssen, J., 2014b. Gully cut-and-fill cycles as related to agro-management: a historical curve number simulation in the Tigray Highlands. Earth Surf. Process. Landf. 40, 796–808.
Lanckriet, S., Rucina, S., Frankl, A., Ritler, A., Gelorini, V., Nyssen, J., 2015. Nonlinear vegetation cover changes in the North Ethiopian Highlands: evidence from the Lake Ashenge closed basin. Sci. Total Environ. (in press).
Lang, A., Mauz, B., 2006. Towards chronologies of gully formation: optical dating of gully fill sediments from Central Europe. Quat. Sci. Rev. 25 (19–20), 2666–2675.
Lehmkuhl, F., Hilgers, A., Fries, S., Hulle, D., Schlutz, F., Shumilovskikh, L., Felauer, T., Protze, J., 2011. Holocene geomorphological processes and soil development as indicator for environmental change around Karakorum, Upper Orkhon Valley (Central Mongolia). Catena 87 (1), 31–44.
Leigh, D.S., Kowalewski, S.A., Holdridge, G.H., 2013. 3400 Years of agricultural engineering in Mesoamerica: Lama-Bordos of the Mixteca Alta, Oaxaca, Mexico. J. Archaeol. Sci. 40, 4107–4111.
Lesur, J., Hildebrand, E., Abawa, G., Gutherz, X., 2014. The advent of herding in the Horn of Africa: new data from Ethiopia, Djibouti and Somaliland. Quat. Int. 343, 148–158.
Machado, M., Pérez-González, A., Benito, G., 1998. Paleoenvironmental changes during the last 4000 yr in the Tigray, Northern Ethiopia. Quat. Res. 49, 312–321.
Marshall, F., Negash, A., 2002. Early hunters and herders of northern Ethiopia: the fauna from Danei Kawlos and Baati Ataro rockshelters. Society for African Archaeologists Meeting (Tucson, Arizona).
Marshall, M., Lamb, H., Davies, S., Leng, M., Kubsa, Zelalem, Umer, M., Bryant, C., 2009. Climatic change in northern Ethiopia during the past 17,000 years: a diatom and stable isotope record from Lake Ashenge. Palaeogeogr. Palaeoclimatol. Palaeoecol. 279, 114–127.
McEvedy, C., Jones, R., 1978. Atlas of World Population History (Hist Atlas). Puffin, London, UK (368 pp.).
Mejdahl, V., 1979. Thermoluminescence dating: beta-dose attenuation in quartz grains. Archaeometry 21, 61–72.
Merla, G., Abbate, E., Azzaroli, A., Bruni, P., Canuti, P., Fazzuoli, M., Sagri, M., Tacconi, P., 1979. A Geological Map of Ethiopia and Somalia (1973). 1:2 000 000; and Comment. University of Florence, Firenze.
Moeyersons, J., Nyssen, J., Poesen, J., Deckers, J., Haile, Mitiku, 2006. Age and backfill/overfill stratigraphy of two tufa dams, Tigray Highlands, Ethiopia: evidence for Late Pleistocene and Holocene wet conditions. Palaeogeogr. Palaeoclimatol. Palaeoecol. 230 (1–2), 165–181.
Murray, A.S., Wintle, A.G., 2000. Luminescence dating of quartz using an improved single-aliquot regenerative-dose protocol. Radiat. Meas. 32, 57–73.
Negash, Tekeste, 2006. The Zagwe period re-interpreted: post-Aksumite Ethiopian urban culture. Afr. Riv. Trimest. Stud. Doc. 61 (1), 120–137.
Nicholson, S., Dezfuli, A., Klotter, D., 2012. A two-century precipitation dataset for the continent of Africa. Am. Meteorol. Soc. http://dx.doi.org/10.1175/BAMS-D-11-00212.1.
Nyssen, J., Poesen, J., Moeyersons, J., Deckers, J., Haile, Mitiku, Lang, A., 2004. Human impact on the environment in the Ethiopian and Eritrean highlands—a state of the art. Earth Sci. Rev. 64 (3–4), 273–320.
Nyssen, J., Poesen, J., Veyret-Picot, M., Moeyersons, J., Haile, Mitiku, Deckers, J., Dewit, J., Naudts, J., Teka, K., Govers, G., 2006. Assessment of gully erosion rates through interviews and measurements: a case study from northern Ethiopia. Earth Surf. Process. Landf. 31 (2), 167–185.
Nyssen, J., Haile, M., Naudts, J., Munro, N., Poesen, J., Moeyersons, J., Frankl, A., Deckers, J., Pankhurst, R., 2009. Desertification? Northern Ethiopia re-photographed after 140 years. Sci. Total Environ. 407, 2749–2755.
Nyssen, J., Frankl, A., Haile, Mitiku, Hurni, H., Descheemaeker, K., Crummey, D., Ritler, A., Portner, B., Nievergelt, B., Moeyersons, J., Munro, R.N., Deckers, J., Billi, P., Poesen, J., 2014. Environmental conditions and human drivers for changes to north Ethiopian mountain landscapes over 145 years. Sci. Total Environ. 485-486, 164–179.
Pankhurst, R., 1990. A Social History of Ethiopia: The Northern and Central Highlands from Early Medieval Times to the Rise of Emperor Tewodros II. Addis Ababa University (371 pp.).
Pankhurst, R., 1997. The Ethiopian Borderlands: Essays in Regional History from Ancient Times to the End of the 18th Century. The Red Sea Press, Asmara, Eritrea.
Pelletier, J., Quade, J., Goble, R., Aldenderfer, M., 2011. Widespread hillslope gullying on the southeastern Tibetan Plateau: human or climate-change induced? Geol. Soc. Am. Bull. 123 (9–10), 1926–1938.
Phillipson, D., 1985. African Archaeology. Cambridge University Press, Cambridge (234 pp.).
Phillipson, D., 2009. The First Millennium BC in the highlands of Northern Ethiopia and South–Central Eritrea: a reassessment of cultural and political development. Afr. Archaeol. Rev. 26, 257–274.
Phillipson, D., 2012. Aksum and the Northern Horn of Africa. Archaeol. Int. 15, 49–52.
Pietsch, D., Machado, M., 2012. Colluvial deposits—proxies for climate change and cultural chronology. A case study from Tigray, Ethiopia. Z. Geomorphol. 58, 119–136 (Supplementary Issues).

Poesen, J., Vandekerckhove, L., Nachtergaele, J., Oostwoud Wijdenes, D., Verstraeten, G., van Wesemael, B., 2002. Gully erosion in dryland environments. In: Bull, L.J., Kirkby, M.J. (Eds.), Dryland Rivers: Hydrology and Geomorphology of Semi-Arid Channels. Wiley, Chichester, UK, pp. 229–262.

Porat, N., Zilberman, E., Amit, R., Enzel, Y., 2001. Residual ages of modern sediments in an hyperarid region, Israel. Quat. Sci. Rev. 20 (5–9), 795–798.

Prescott, J.R., Hutton, J.T., 1994. Cosmic ray contributions to dose rates for luminescence and ESR dating: large depths and long-term time variations. Radiat. Meas. 23, 497–500.

Sagri, M., Bartolini, C., Billi, P., Ferrari, G., Benvenuti, M., Carnicelli, S., Barbano, F., 2008. Latest Pleistocene and Holocene river network evolution in the Ethiopian Lakes Region. Geomorphology 94, 79–97.

Schütt, B., Frechen, M., Hoelzmann, P., Fritzenwenger, G., 2011. Late Quaternary landscape evolution in a small catchment on the Chinese Loess Plateau. Quat. Int. 234, 159–166.

Shaw, A., Holmes, P., Rogers, J., 2001. Depositional landforms and environmental change in the headward vicinity of Dias Beach, Cape Point. S. Afr. J. Geol. 101 (2), 101–114.

Summa-Nelson, M., Rittenour, T., 2012. Application of OSL dating to middle to late Holocene arroyo sediments in Kanab Creek, southern Utah, USA. Quat. Geochronol. 10, 167–174.

Teeuw, R., Rhodes, E., Perkins, N., 1999. Dating of quaternary sediments from western Borneo, using optically stimulated luminescence. Singap. J. Trop. Geogr. 20 (2), 181–192.

Terwilliger, V.J., Eshetu, Z., Huang, Y., Alexandre, M., Umer, M., Gebru, T., 2011. Local variation in climate and land use during the time of the major kingdoms of the Tigray Plateau in Ethiopia and Eritrea. Catena 85, 130–143.

Thomas, M., Murray, A., 2001. On the age and significance of Quaternary colluvium in eastern Zambia. Palaeoecol. Afr. 27, 117–133.

Tooth, S., Hancox, P., Brandt, D., McCarthy, T., Jacobs, Z., Woodborne, S., 2013. Controls on the genesis, sedimentary architecture, and preservation potential of dryland alluvial successions in stable continental interiors: insights from the incising Modder River, South Africa. J. Sediment. Res. 83 (7–8), 541–561.

Vanmaercke, M., Poesen, J., Verstraeten, G., Maetens, W., de Vente, J., 2011. Sediment yield as a desertification risk indicator. Sci. Total Environ. 409, 1715–1725.

Vanmaercke, M., Poesen, J., Broeckx, J., Nyssen, J., 2014. Sediment yield in Africa. Earth Sci. Rev. 136, 350–368.

Wallinga, J., 2002. Optically stimulated luminescence dating of fluvial deposits: a review. Boreas 31 (4), 303–322.

Wintle, A.G., Murray, A.S., 2006. A review of quartz optically stimulated luminescence characteristics and their relevance in single-aliquot regeneration dating protocols. Radiat. Meas. 41, 369–391.

Zimmerman, D.W., 1971. Thermoluminescent dating using fine grains from pottery. Archaeometry 13, 29–50.